Journal of Quantitative Spectroscopy & Radiative Transfer 34 (2020) 107215

Contents lists available at ScienceDirect

Journal of Quantitative Spectroscopy & Radiative Transfer

journal homepage: www.elsevier.com/locate/jqsrt

Resonance enhanced two-photon ionization spectrum of ultracold $^{85}Rb^{133}Cs$ molecules in $(2)^1\Pi_1 \leftarrow X^1\Sigma^+$ transitions

Zhonghua Ji[a,b,*], Ting Gong[a,b], Yanting Zhao[a,b,*], Chuanliang Li[c], Liantuan Xiao[a,b], Suotang Jia[a,b]

[a] State Key Laboratory of Quantum Optics and Quantum Optics Devices, Institute of Laser Spectroscopy, Shanxi University, Taiyuan 030006, China
[b] Collaborative Innovation Center of Extreme Optics, Shanxi University, Taiyuan, Shanxi 030006, China
[c] Department of Physics, School of Applied Science, Taiyuan University of Science and Technology, Taiyuan 030024, China

ARTICLE INFO

Article history:
Received 16 May 2020
Revised 9 July 2020
Accepted 11 July 2020
Available online 13 July 2020

Keywords:
Ultracold molecule
RETPI Spectrum
Photoassociation
Franck-Condon factor
RbCs

ABSTRACT

We present resonance enhanced two-photon ionization (RETPI) spectrum between 14,500 and 15850 cm^{-1} for ultracold ground state $^{85}Rb^{133}Cs$ molecules. With an assistant of optical pumping from one 1070nm laser, $(2)^1\Pi_1 \leftarrow X^1\Sigma^+$ electronic transition is distinguished from $(4)^3\Sigma^+ \leftarrow a^3\Sigma^+$ and $(3)^3\Pi \leftarrow a^3\Sigma^+$ transitions. Some observed RETPI spectra are globally assigned to vibrational transitions from $X^1\Sigma^+(v = 0-5)$ to $(2)^1\Pi_1(v = 5-20)$. Based on these assignments, the spectroscopic constants of $X^1\Sigma^+$ and $(2)^1\Pi_1$ are simultaneously derived, including energy separation, harmonic and anharmonic constants. Then a map of Franck-Condon factors between vibrational transitions of $X^1\Sigma^+(v = 0-9)$ and $(2)^1\Pi_1(v = 0-20)$ is plotted based on these constants. Our present work would be meaningful for continuous accumulation of ultracold $^{85}Rb^{133}Cs$ molecules in the lowest vibronic state with further optical pumping.

1. Introduction

Ultracold polar molecules have attracted great interests for both physicists and chemists due to their rich rovibrational structures, large permanent electric dipole moments and long coherent times [1–5]. These characteristics allow potential applications in ultracold chemistry [6,7], quantum computation [8,9], quantum simulation [10,11], precise measurement [12,13] and degenerate quantum gas [14].

All of these applications require efficient production of molecules in a well-defined ground state. Up to now such molecules may be produced in a variety of ways. One approach is to transfer pairs of ultracold atoms to a Feshbach state by ramping a magnetic field, and then coherently transfer to a vibronic level of molecular state by implementing stimulated Raman adiabatic passage [15]. In favourable cases, this method can produce molecules in a single hyperfine and Zeeman state [16–22]. However, this approach produce molecules only once during one experimental cycle, which usually takes around one minute. Contrastively, other two alternative approaches, direct laser cooling [23] and short-range photoassociation (PA) [24] allow continuously producing molecules. The former method has a rapid develop recently with a milestone of realizing molecular magneto-optical trapping [25–27]. As this method requires nearly closed laser-cooling transitions, it is still limited to a small class of molecules. The latter depends on resonant coupling of PA excited states, which have both appropriate Franck-Condon (F-C) factors with initially scattering atomic state and deeply bound molecular state. In short-range PA, the formed molecules are distributed in several vibrational levels, that is unfavorable for producing a pure quantum state. If transition information between the distributed ground state and an suitable excited state can be obtained, it can provide guides for implementing optical pumping to continuously accumulate molecules in one pure quantum state, just like the case of homonuclear Cs_2 molecules [28].

In 2010 Stwalley *et al.* theoretically studied resonant coupling states for short-range PA in all 10 heteronuclear alkali metal dimers [24]. Since then such approach has been implemented in LiCs [29], NaCs [30], KRb [31], RbCs [32] and LiRb [33]. Among these dimers, RbCs molecule, especially $^{85}Rb^{133}Cs$, attract interests benefiting from its special characteristics: sizable permanent electric dipole moment [34] enables easy alignment for quantum simulation [11]; avoidable immiscibility of its components, which is different from its isotopic components [35], provides possibility to realize molecular Bose-Einstein condensation; inelastic colli-

* Corresponding author at: Shanxi University Wucheng Road 92, Taiyuan, Shanxi 030006, China.
E-mail addresses: jzh@sxu.edu.cn (Z. Ji), zhaoyt@sxu.edu.cn (Y. Zhao).

https://doi.org/10.1016/j.jqsrt.2020.107215
0022-4073/

sion with co-trapped Cs atom also supports molecule purification in lowest vibronic state [36].

In Ref[24]., the authors proposed that $(2)^1\Pi_1$ electronic state, which has resonant coupling with $(1)^1\Pi_1$ (or $(B)^1\Pi_1$) state, appears to be a quite promising path for producing ultracold RbCs molecules in the lowest vibronic ground state. Over the past ten years, several short-range PA electronic states [32,37–45], including the early proposed $(2)^1\Pi_1$ state [43], were used to produce ultracold ground state $^{85}Rb^{133}Cs$ molecules. Reference [43] also shows that most vibrational levels of $2^1\Pi_1$ state have relatively strong production rates, indicating that this state may provide a promising passway to implement optical pumping. Thus transition information between $(2)^1\Pi_1$ and $X^1\Sigma^+$ states is required.

It is known that resonance enhanced two-photon ionization (RETPI) spectroscopy is an easy and quick method to obtain such information. In 2014 Bruzewicz *et al.* presented a portion of $(2)^1\Pi \leftarrow X^1\Sigma^+$ RETPI spectrum for RbCs molecules. The scanning range of photoionization (PI) laser frequency is 15180–15340 cm^{-1}. They found that the formed molecules mainly distributed in $X^1\Sigma^+(v = 0-5)$ levels. Except for the lowest vibronic state, other vibrational transitions are not assigned in that work. The finite assignments are insufficient to derive transition information between $(2)^1\Pi_1$ and $X^1\Sigma^+$ states.

In this paper, the RETPI spectrum of ultracold ground state $^{85}Rb^{133}Cs$ molecules with a larger frequency range between 14,500 and 15850 cm^{-1} is presented. With an assistant of optical pumping from a 1070nm laser, three electronic transitions, $(4)^3\Sigma^+ \leftarrow a^3\Sigma^+$, $(2)^1\Pi_1 \leftarrow X^1\Sigma^+$ and $(3)^3\Pi \leftarrow a^3\Sigma^+$ are distinguished. On the focused $2^1\Pi_1 \leftarrow X^1\Sigma^+$ transition where the formed molecules are excited from the single ground state, vibrational transitions among $(2)^1\Pi(v = 5-20) \leftarrow X^1\Sigma^+(v = 0-5)$ are assigned. The energy separation between these two electronic states T_e, harmonic constant ω and anharmonic constants $\omega\chi$ for each state, ωy for $(2)^1\Pi_1$ state, are derived simultaneously. Based on these derived spectroscopic constants, a map of F-C factors is plotted. These investigations would be meaningful for accumulating $^{85}Rb^{133}Cs$ molecules in the lowest vibronic ground state with further optical pumping.

2. Experimental setup

Our experimental setup and operation procedure are nearly the same as one of our publications [47], in which RETPI spectrum between 13,700 and 14600 cm^{-1} of ultracold RbCs molecules was reported. In that paper molecules in the metastable ground state $a^3\Sigma^+$ are photoionized, while here molecules lay in the single ground state $X^1\Sigma^+$.

Fig. 1 shows the formation and detection mechanisms of ultracold ground state $^{85}Rb^{133}Cs$ molecules we use. In a vacuum chamber with a pressure of 3×10^{-6} Pa, 1×10^7 ^{85}Rb atoms in $5S_{1/2}$ $(F = 2)$ state with a density of 8×10^{10} cm^{-3} and 2×10^7 ^{133}Cs atoms in $6S_{1/2}$ $(F = 3)$ state with a density of 1.5×10^{11} cm^{-3} were produced using a space-adjustable dual-species dark spontaneous force optical traps. Colliding atomic pair of ^{85}Rb and ^{133}Cs were photoassociated into $2^3\Pi_{0^+}(v = 10, J = 2)$ level which is adiabatically correlated to $Rb(5P_{3/2})$+$Cs(6S_{1/2})$ dissociation limit at long range [41]. The molecules in this level is not stable and will soon decays to the $X^1\Sigma^+$ and $a^3\Sigma^+$ states, including but not only $X^1\Sigma^+(v = 0)$ level. The formed molecules are then excited by a pulsed dye laser to vibrational levels of higher electronic states, containing $(4)^3\Sigma^+$, $(2)^1\Pi_1$ and $(3)^3\Pi$ in this work. The specific transitions depend on dye laser frequency. With the Dichloromethane (DCM) molecule in a solvent of Dimethylsulfoxide (DMSO) we used, laser frequency can cover around 14000–16000 cm^{-1}. Once excited, these molecules were photoionized by a 532 nm laser and detected by a pair of microchannel plates (MCPs) under a pulsed electric field. After amplification, the acquired signal was integrated and averaged by a Boxcar (SRS-250) every 10 shots.

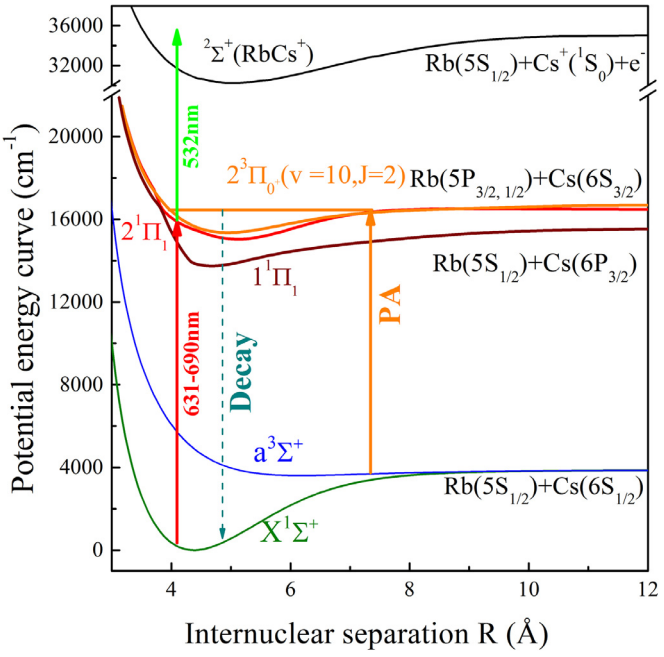

Fig. 1. Formation and detection mechanisms of ultracold ground state $^{85}Rb^{133}Cs$ molecules. The potential energy curves (PEC) come from Ref[46].

3. Results

Fig. 2(a) shows our measured RETPI spectrum between 14,500 and 15850 cm^{-1} of ultracold RbCs molecules formed via $2^3\Pi_{0^+}(v = 10, J = 2)$ rovibrational level. The PI laser frequency is scanned with a speed of 0.04 nm/s. As the linewidth of dye laser is 3 GHz and rotational constant of RbCs molecules in ground state is around 500 MHz [48], RETPI can only resolve vibrational transitions. Even there were published abundant literatures on structures and spectra of RbCs molecule, accurate assignments for such a spectrum are still challenging because that vibrational transitions of different electronic transitions may mix with each other.

In our experiment we have a 1070 nm broadband fiber laser (IPG Photonics, YLR-300-AC) with an initial aim to optically trap the formed molecules [49]. It is accidental to find that this laser can strongly change vibrational distributions of the formed molecules, even the beam is unfocused and the intensity is low. Fig. 2(b) shows our measured spectrum under the same conditions of Fig. 2(a) but in the presence of one 1070 nm beam with a diameter of around 500 μm and a power of around 100 mW. Comparing with Fig. 2(a), we find that molecular ion intensity in Fig. 2(b) increases below 15600 cm^{-1} but decreases over this value. The different tendency of molecule production exclude 1070 nm laser-induced PA. We attribute this vibrational redistribution to optically pumping of RbCs molecules. Considering the frequency of this optically pumping laser, the formed RbCs molecules in $a^3\Sigma^+$ state may be excited to $c^3\Sigma^+_{0^-,1}$ state, which mixes with $b^3\Pi_{0^+,0^-,1,2}$ and $B^1\Pi_1$ states [50], and spontaneously decay to lower vibrational levels of single and triplet ground states. As the linewidth of 1070nm laser is large as 2 nm and vibrational distribution of formed molecules in $a^3\Sigma^+$ state is uncertainty, it is impossible to address particular vibrational transitions.

With the observed vibrational redistribution in mind, we divide this RETPI spectrum to three parts, separated with green

Table 1
Spectroscopic constants of RbCs molecules in $X^1\Sigma^+$ and $(2)^1\Pi_1$ states. The unit is cm^{-1}.

	$X^1\Sigma^+$		$(2)^1\Pi_1$			
References	ω_g	$\omega\chi_g$	T_e	ω_e	$\omega\chi_e$	ωy_e
Theo [60].	45.6	-	15003	40.33	-	-
Theo [46].	51.35	-	15046	33.36	-	-
Theo [61].	51.3	-	15039	35.2	-	-
Theo [62].	-	-	14987	33.1	-	-
Theo [63].	49.09	-	15287	30.72	-	-
Theo [64].	50.23	0.105	15077	32.98	0.0165	-
Expt [57].	50.01	0.109	-	-	-	-
Expt [59].	-	-	14963.62	32.93	0.025	-0.0023
Expt [58].	50.01	0.1095	-	-	-	-
This work	50.00(7)	0.11(1)	14964.4(7)	32.68(19)	0.013(16)	-0.0023(4)

dashes in Fig. 2. The electronic transition of left part (roughly from 14,500 to 14930 cm^{-1}) is assigned to $(4)^3\Sigma^+ \leftarrow a^3\Sigma^+$, middle part (14930 to 15570 cm^{-1}) to $(2)^1\Pi_1 \leftarrow X^1\Sigma^+$ and right part (15570 to 15850 cm^{-1}) to $(3)^3\Pi \leftarrow a^3\Sigma^+$. The main basis of these assignments comes from Ref[51]., in which some absorption bands of RbCs molecules under cold condition is calculated. In the Fig. 2 of Ref[51]., the authors calculated FC factors between the lowest vibrational states of the ground states (containing triplet $a^3\Sigma^+$ and single $X^1\Sigma^+$ state) and the allowed vibrational states of the lowest four excited states (containing $^1\Sigma^+$, $^3\Sigma^+$, $^1\Pi$, $^3\Pi$) under a temperature of 0.4 K. These calculations are strongly referenced for RETPI spectra in cold molecular beam and short-range PA experiments, where molecules distribute in low vibrational levels. The authors have verified the reliability of their calculations by taking $(3)^1\Pi \leftarrow X^1\Sigma^+$ RETPI spectrum as an example [52]. Besides of this transition, electronic transitions of $(4)^1\Sigma^+ \leftarrow X^1\Sigma^+$ [52] and $(5)^1\Sigma^+ \leftarrow X^1\Sigma^+$ [53] are also agreeable with their calculations.

In these three transitions we are specially interested in $(2)^1\Pi \leftarrow X^1\Sigma^+$. Besides of the mentioned Ref [40]. in the introduction part, the RETPI spectrum in cold molecular beam [54,55] also provide a basis for our assignment by addressing $(2)^1\Pi(v = 11-21) \leftarrow X^1\Sigma^+(v = 0)$ vibrational transitions. However, all of these literatures assigned vibrational transition from only $X^1\Sigma^+(v = 0)$ level. To address all vibrational transitions, it is necessary to have a global assignment by simultaneously deriving spectroscopic constants for these two electronic states.

As our obtained RETPI spectrum only has vibrational resolution, the energy expression for molecules can be written as [56]

$$E/hc = \sum_i Y_{i0}\left(v + \frac{1}{2}\right)^i \tag{1}$$

where v is vibrational number, h is the Planck constant, c is the speed of light, Y_{i0} is Dunham coefficient for vibrational terms in which Y_{00} is the minimum point of PEC of electric state and other coefficients can be established relationships to conventional spectroscopic constants (*e.g.* Y_{10}, Y_{20} and Y_{30} correspond harmonic constant ω, anharmonic constants $-\omega\chi$ and ωy respectively). The Table 1 of both Refs [57]. and [58] shows that for $X^1\Sigma^+$ state Y_{i0} with $i \geq 3$ are smaller than Y_{20} by at least of 3 orders of magnitude, while for $(2)^1\Pi_1$ state Y_{i0} with $i \geq 4$ smaller than Y_{20} with the same magnitude, shown in Ref [59]. Here we ignore these tiny coefficients on the condition of large uncertainty in our RETPI spectrum. By convention we choose the minimum point of the $X^1\Sigma^+$ PEC as reference point (*i.e.* T_g=0), then transition energy between $X^1\Sigma^+$ and $(2)^1\Pi_1$ states is simplified as

$$E/hc = T_e + \omega_e\left(v_e + \frac{1}{2}\right) - \omega\chi_e\left(v_e + \frac{1}{2}\right)^2 + \omega y_e\left(v_e + \frac{1}{2}\right)^3 - \omega_g\left(v_g + \frac{1}{2}\right) + \omega\chi_g\left(v_g + \frac{1}{2}\right)^2. \tag{2}$$

Based on this equation and the previous literatures [40,54,55], we assign 76 vibrational transitions among $(2)^1\Pi_1(v = 5-20)$ states, shown in Fig. 3. We use different color lines to discriminate different vibrational series of ground state and for simplify we only label the vibrational numbers of excited states at two ends for each serie. All the values of vibrational transitions can be found in Supplemental Material. The uncertainty of frequency value is around 0.3 cm^{-1} after considering the linewidth of PI laser and fluctuation of photoionized signal. Those peaks unassigned from the start of shown spectrum seem regular and are possible to belong to vibrational transition of the nearby $(4)^3\Sigma^+ \leftarrow a^3\Sigma^+$ electronic transition. But it is difficulty to specify accurate transition and it is also out of the theme of this work.

After assignments, we fit all the observed transitions with Eq. (2) and list the derived spectroscopic constants in Table 1, along with other available theoretical calculations [46,60–64] and experimental measurements [57–59]. Experiments in Refs [57–59]. implemented laser-induced fluorescence of hot RbCs molecules in a heat-pipe. There are abundant uncontrolled vibrational transitions with many high rotational numbers in this kind of experiment. That make spectrum analysis complicated because that energy with low vibrational number and high rotational number may be larger than the energy with the contrary case. In contrast, the vibrational transition in RETPI spectrum we use can be easily chosen by laser frequency and there is no existence of high rotational transition. It is also convenient to simultaneously obtain spectroscopic constants for both $X^1\Sigma^+$ and $(2)^1\Pi_1$ states. The fitting values in this work show well consistences with other available experimental measurements in view of measured uncertainty, except for ωy_e which we attribute the deviation to the lacks of coupled terms between vibrational and rotational angular moment (see the F(J) expression in table 3 in Ref. [59]). Once obtaining spectroscopic constants, one can easily obtain the predicted values by substituting these constants to Eq. (2). In the Supplemental Material we have listed the residuals of observations from the predicted values. Most residuals lay in less than 0.5 cm^{-1}, even there are four relative large deviations around 2 cm^{-1} exist. The uncertainty mainly comes from perturbation between vibrational transitions, large linewidth from dye laser, power fluctuation and the absence of high terms in Eq. (1) that not included in Eq. (2).

Based on these derived spectroscopic constants, it is possible to generate a Rydberg-Klein-Rees (RKR) PEC for both $X^1\Sigma^+$ and $(2)^1\Pi_1$ states by using LeRoys RKR1 program [65], shown in Fig. 4. To make a comparison, we also add PECs of these two states calculated in Ref [46]. The inner potential wall has been corrected by the RKR1 program. The reference level of electronic energy is the minimum value of the potential well of $X^1\Sigma^+$ ground state. It is shown and unsurprised that the deviation of theoretical calculation from experimental measurement is larger for $(2)^1\Pi_1$ excited state than the case of ground state. As the RETPI spectroscopy re-

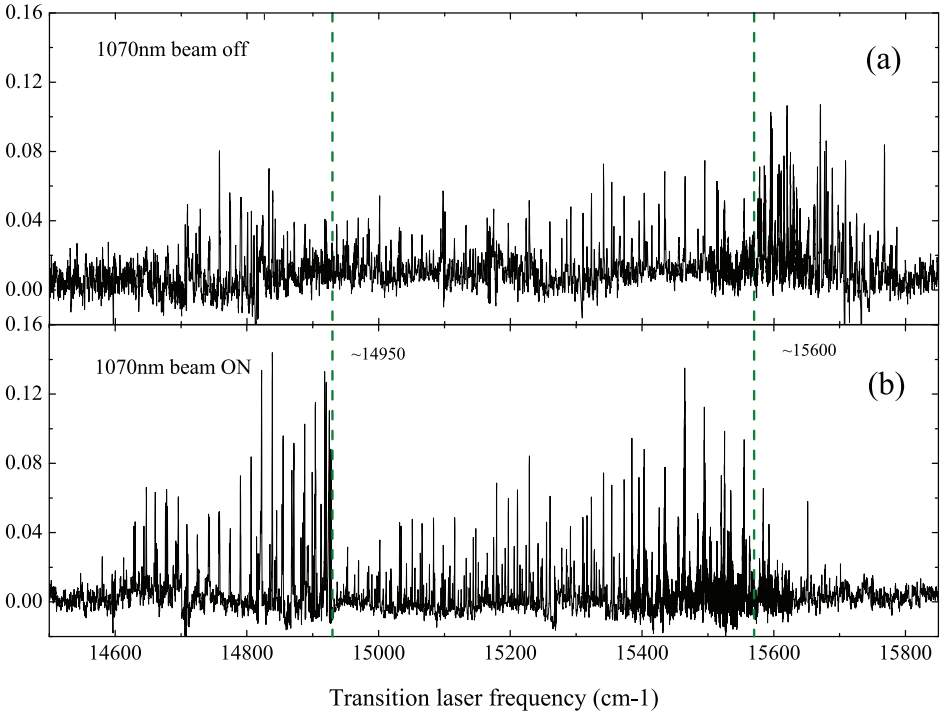

Fig. 2. RETPI spectrum of RbCs molecules between 14,500 and 15850 cm^{-1} in the absence (a) and presence (b) of one 1070nm beam. The electronic transitions of left, central and right parts (separated with green dashes) are assigned to $(4)^3\Sigma^+ \leftarrow a^3\Sigma^+$, $(2)^1\Pi_1 \leftarrow X^1\Sigma^+$ and $(3)^3\Pi \leftarrow a^3\Sigma^+$ respectively. (For interpretation of the references to colour in this figure legend, the reader is referred to the web version of this article.)

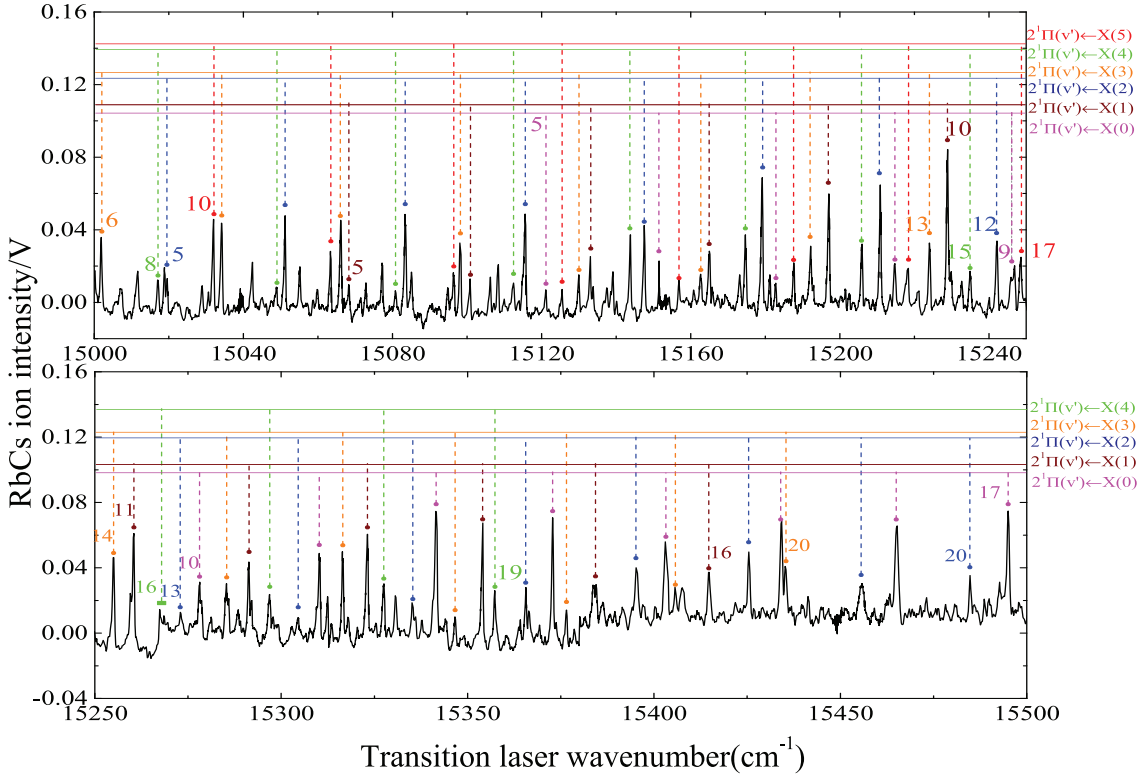

Fig. 3. Enlargement of Fig. 2(b) between 15000–15500 cm^{-1}. There are 76 assigned vibrational transitions among $(2)^1\Pi_1(v = 5 - 20)$ and $X^1\Sigma^+(v = 0 - 5)$ states. Different color lines discriminate different vibrational series of ground state and for simplify we only label the vibrational numbers at two ends of each serie.

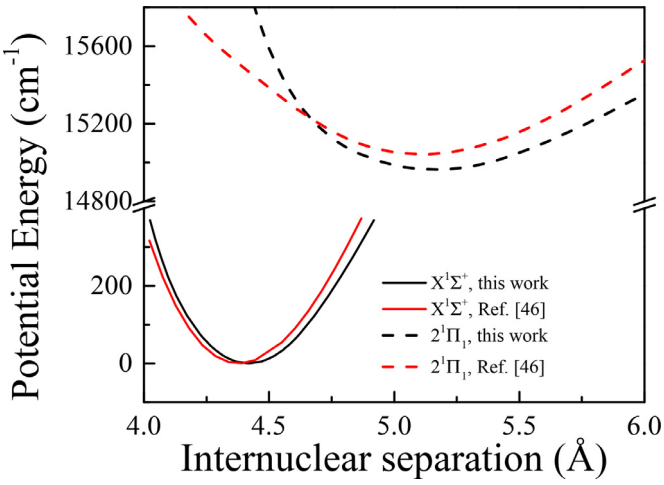

Fig. 4. The obtained RKR PECs of $(2)^1\Pi_1$ (dashes) and $X^1\Sigma^+$ electronic states (lines). The red curves indicate the values calculated by RKR method while the black for the *ab initio* values from Ref [46]. The energy is relative to the lowest PEC of $X^1\Sigma^+$ electronic state. (For interpretation of the references to colour in this figure legend, the reader is referred to the web version of this article.)

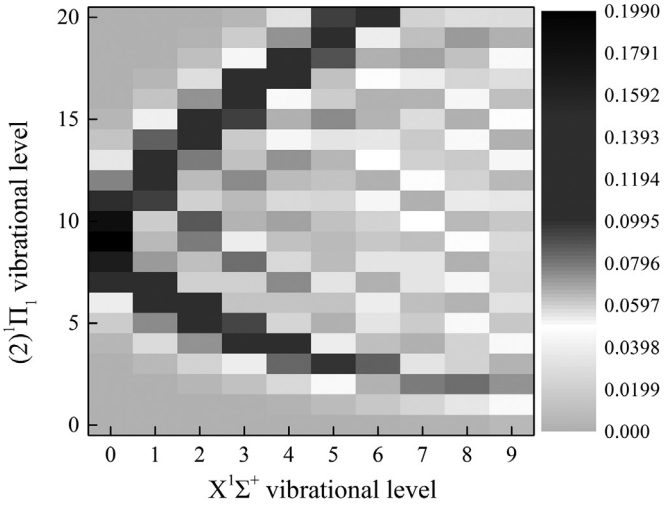

Fig. 5. F-C factors of vibrational transitions between $X^1\Sigma^+(v=0-9)$ and $(2)^1\Pi_1(v=0-25)$.

flects directly transition information between coupled two states, we are confident with our derived PEC.

With the revised PECs of $(2)^1\Pi_1$ and $X^1\Sigma^+$ states, we can further quantify transition probability for their transition. Fig. 5 sketches the F-C factors of vibrational transitions for $(2)^1\Pi(v=0-20)-X^1\Sigma^+(v=0-9)$ of $^{85}Rb^{133}Cs$ molecules. Numerical values are listed in the Supplemental Material. It is presented that the local optimal values in this graph distribute in a $<$ shape. Even the upper part of $<$ shape has larger values than the bottom portion, the bottom part of $<$ shape should be used when one would implement optical pumping for that it can avoid redistribution of higher vibrational levels.

4. Conclusions

The RETPI spectrum of ultracold ground state $^{85}Rb^{133}Cs$ molecules between 14,500 and 15850 cm^{-1} has been investigated. Optical pumping from one 1070 nm laser is used to distinguish $(4)^3\Sigma^+\leftarrow a^3\Sigma^+$, $(2)^1\Pi_1\leftarrow X^1\Sigma^+$ and $(3)^3\Pi\leftarrow a^3\Sigma^+$ electronic transitions. Vibrational transitions among $(2)^1\Pi_1(v=5-20)\leftarrow X^1\Sigma^+(v=0-5)$ have been assigned. Based on these assignments, the following spectroscopic constants have been obtained simultaneously for both $X^1\Sigma^+$ and $(2)^1\Pi_1$ states: harmonic constant ω and anharmonic constants $\omega\chi$ for each state, ωy for $(2)^1\Pi_1$ state. These spectroscopic constants allows us to plot a F-C factors map between vibrational transitions of $X^1\Sigma^+(v=0-9)$ and $(2)^1\Pi_1(v=0-20)$. That would be meaningful for accumulating absolute ground state molecules with further optical pump.

Declaration of Competing Interest

The auithors declare that they have no known competing financial interests or personel relationships that could have appeared to influence the work reported in this paper.

CRediT authorship contribution statement

Zhonghua Ji: Conceptualization, Methodology, Investigation, Writing - original draft. **Ting Gong:** Investigation, Data curation. **Yanting Zhao:** Investigation, Writing - review & editing, Funding acquisition. **Chuanliang Li:** Software, Visualization. **Liantuan Xiao:** Funding acquisition. **Suotang Jia:** Funding acquisition.

Acknowledgement

This work was supported by National Key Research and Development Program of China (Grant No. 2017YFA0304203), Natural Science Foundation of China (Nos. 61675120, 61875110), NSFC Project for Excellent Research Team (No. 61121064), Shanxi "1331 Project" Key Subjects Construction, PCSIRT (No. IRT_17R70), 111 project (Grant No. D18001).

Supplementary material

Supplementary material associated with this article can be found, in the online version, at 10.1016/j.jqsrt.2020.107215

References

[1] Dulieu O, Krems R, Weidemüller M, Willitsch S. Physics and chemistry of cold molecules. Phys Chem Chem Phys 2011;13:18703. doi:10.1039/C1CP90157E.
[2] Quéméner G, Julienne PS. Ultracold molecules under control!. Chem Rev 2012;112:4949. doi:10.1021/cr300092g.
[3] Ulmanis J, Deiglmayr J, Repp M, Wester R, Weidemüller M. Ultracold molecules formed by photoassociation: heteronuclear dimers, inelastic collisions, and interactions with ultrashort laser pulses. Chem Rev 2012;112:4890. doi:10.1021/cr300215h.
[4] Moses SA, Vovey JP, Miecnikowski MT, Jin DS, Ye J. New frontiers for quantum gases of polar molecules. Nat Phys 2017;13:13. doi:10.1038/nphys3985.
[5] Bohn JL, Rey AM, Ye J. Cold molecules: progress in quantum engineering of chemistry and quantum matter. Science 2017;357:1002. doi:10.1126/science.aam6299.
[6] Krems RV. Cold controlled chemistry. Phys Chem Chem Phys 2008;10:4079. doi:10.1039/B802322K.
[7] Ospelkaus S, Ni K-K, Wang D, de Miranda MHG, Neyenhuis B, Quéméner G, et al. Quantum-state controlled chemical reactions of ultracold potassium-rubidium molecules. Science 2010;327:853. doi:10.1126/science.1184121.
[8] DeMille D. Quantum computation with trapped polar molecules. Phys Rev Lett 2002;88:067901. doi:10.1103/PhysRevLett.88.067901.
[9] Ni K-K, Rosenband T, Grimes DD. Dipolar exchange quantum logic gate with polar molecules. Chem Sci 2018;2355:1039. doi:10.1039/c8sc02355g.
[10] Georgescu IM, Ashhab S, Nori F. Quantum simulation. Rev Mod Phys 2014;86:153. doi:10.1103/RevModPhys.86.153.
[11] Blackmore JA, Caldwell L, Gregory PD, Bridge EM, Sawant R, Aldegunde J, et al. Ultracold molecules for quantum simulation: rotational coherences in CaF and RbCs. Quantum Sci Technol 2018;4:014010. doi:10.1088/2058-9565/aaee35.
[12] Chin C, Flambaum VV, Kozlov MG. Ultracold molecules: new probes on the variation of fundamental constants. New J Phys 2009;11:055048. doi:10.1088/1367-2630/11/5/055048.
[13] Wall TE. Preparation of cold molecules for high–precision measurements. J Phys B: At Mol Opt Phys 2016;49:243001. doi:10.1088/0953-4075/49/24/243001.
[14] De Marco L, Valtolina G, Matsuda K, Tobias WG, Covey JP, Ye J. A degenerate fermi gas of polar molecules. Science 2019;363:853. doi:10.1126/science.aau7230.

[15] Vitanov NV, Rangelov AA, Shore BW, Bergmann K. Stimulated raman adiabatic passage in physics, chemistry, and beyond. Rev Mod Phys 2017;89:015006. doi:10.1103/RevModPhys.89.015006.

[16] Ni K-K, Ospelkaus S, de Mirandal MHG, Péer A, Neyenhuis B, Zirbel JJ, et al. A high phase-space-density gas of polar molecules. Science 2008;322:231. doi:10.1126/science.1163861.

[17] Takekoshi T, Reichsöllner L, Schindewolf A, Hutson JM, Le Sueur CR, Dulieu O, et al. Ultracold dense samples of dipolar RbCs molecules in the rovibrational and hyperfine ground state. Phys Rev Lett 2014;113:205301. doi:10.1103/PhysRevLett.113.205301.

[18] Molony PK, Gregory PD, Ji Z, Lu B, Köppinger MP, Le Sueur CR, et al. Creation of ultracold $^{87}Rb^{133}Cs$ molecules in the rovibrational ground state. Phys Rev Lett 2014;113:255301. doi:10.1103/PhysRevLett.113.255301.

[19] Park JW, Will SA, Zwierlein MW. Ultracold dipolar gas of fermionic $^{23}Na^{40}K$ molecules in their absolute ground state. Phys Rev Lett 2015;114:205302. doi:10.1103/PhysRevLett.114.205302.

[20] Guo M, Zhu B, Lu B, Ye X, Wang F, Vexiau R, et al. Creation of an ultracold gas of ground-state dipolar $^{23}Na^{87}Rb$ molecules. Phys Rev Lett 2016;116:205303. doi:10.1103/PhysRevLett.116.205303.

[21] Rvachov TM, Son H, Sommer AT, Ebadi S, Park JJ, Zwierlein MW, et al. Long-lived ultracold molecules with electric and magnetic dipole moments. Phys Rev Lett 2017;119:143001. doi:10.1103/PhysRevLett.119.143001.

[22] Yang A, Botsi S, Kumar S, Pal SB, Lam MM, Čepaitė I, et al. Singlet pathway to the ground state of ultracold polar molecules. Phys Rev Lett 2020;124:133203. doi:10.1103/PhysRevLett.124.133203.

[23] Tarbutt MR. Laser cooling of molecules. Contemp Phys 2018;59:356. doi:10.1080/00107514.2018.1576338.

[24] Stwalley WC, Banerjee J, Bellos M, Carollo R, Recore M, Mastroianni M. Resonant coupling in the heteronuclear alkali dimers for direct photoassociative formation of x(0,0) ultracold molecules. J Phys Chem A 2010;114:81. doi:10.1021/jp901803f.

[25] Barry JF, McCarron DJ, Borrgard EB, Steinecker MH, DeMille D. Magneto-optical trapping of a diatomic molecule. Nature 2014;512:286. doi:10.1038/nature13634.

[26] Truppe S, Williams HJ, Caldwell L, Fitch NJ, Hinds EA, Sauer BE, et al. Molecules cooled below the doppler limit. Nat Phys 2017;13:1173. doi:10.1038/nphys4241.

[27] Anderegg L, Augenbraun BL, Chae E, Hemmerling B, Hutzler NR, Ravi A, et al. Radio frequency magneto-optical trapping of CaF with high density. Phys Rev Lett 2017;119:103201. doi:10.1103/PhysRevLett.119.103201.

[28] Viteau M, Chotia A, Allegrini M, Bouloufa N, Dulieu O, Comparat D, et al. Optical pumping and vibrational cooling of molecules. Science 2008;321:232. doi:10.1126/science.1159496.

[29] Deiglmayr J, Grochola A, Repp M, Mörtlbauer K, Glück C, Lange J, et al. Formation of ultracold polar molecules in the rovibrational ground state. Phys Rev Lett 2008;101:133004. doi:10.1103/PhysRevLett.101.133004.

[30] Zabawa P, Wakim A, Haruza M, Bigelow NP. Formation of ultracold $X^1\Sigma^+(v''=0)$ NaCs molecules via coupled photoassociation channels. Phys Rev A 2011;84:061401(R). doi:10.1103/PhysRevA.84.061401.

[31] Banerjee J, Rahmlow D, Carollo R, Bellos M, Eyler EE, Gould PL, et al. Direct photoassociative formation of ultracold KRb molecules in the lowest vibrational levels of the electronic ground state. Phys Rev A 2012;86:053428. doi:10.1103/PhysRevA.86.053428.

[32] Shimasaki T, Bellos M, Bruzewicz CD, Lasner Z, DeMille D. Production of rovibronic-ground-state RbCs molecules via two-photon-cascade decay. Phys Rev A 2015;91:021401. doi:10.1103/PhysRevA.91.021401.

[33] Stevenson IC, Blasing DB, Chen YP, Elliott DS. Production of ultracold ground-state LiRb molecules by photoassociation through a resonantly coupled state. Phys Rev A 2016;94:062510. doi:10.1103/PhysRevA.94.062510.

[34] Aymar M, Dulieu O. Calculation of accurate permanent dipole moments of the lowest $^{1,3}\Sigma^+$ states of heteronuclear alkali dimers using extended basis sets. J Chem Phys 2005;122. doi:10.1063/1.1903944.

[35] McCarron DJ, Cho HW, Jenkin DL, Köppinger MP, Cornish SL. Dual-species bose-einstein condensate of ^{87}Rb and ^{133}Cs. Phys Rev A 2011;84:011603. doi:10.1103/PhysRevA.84.011603.

[36] Hudson ER, Gilfoy NB, Kotochigova S, Sage JM, DeMille D. Inelastic collisions of ultracold heteronuclear molecules in an optical trap. Phys Rev Lett 2008;100:203201. doi:10.1103/PhysRevLett.100.203201.

[37] Gabbanini C, Dulieu O. Formation of ultracold metastable RbCs molecules by short-range photoassociation. Phys Chem Chem Phys 2011;13:18905. doi:10.1039/C1CP21497G.

[38] Ji Z, Zhang H, Wu J, Yuan J, Yang Y, Zhao Y, et al. Photoassociative formation of ultracold rbcs molecules in the $(2)^3\Pi$ state. Phys Rev A 2012;85:013401. doi:10.1103/PhysRevA.85.013401.

[39] Fioretti A, Gabbanini C. Experimental study of the formation of ultracold RbCs molecules by short-range photoassociation. Phys Rev A 2013;87:054701. doi:10.1103/PhysRevA.87.054701.

[40] Bruzewicz CD, Gustavsson M, Shimasaki T, DeMille D. Continuous formation of vibronic ground state RbCs molecules via photoassociation. New J Phys 2014;16:023018. doi:10.1088/1367-2630/16/2/023018.

[41] Yuan J, Zhao Y, Ji Z, Li Z, Kim J-T, Xiao L, et al. The determination of potential energy curve and dipole moment of the $(5)0^+$ electronic state of $^{85}Rb^{133}Cs$ molecule by high resolution photoassociation spectroscopy. J Chem Phys 2015;143:224312. doi:10.1063/1.4936914.

[42] Zhao Y, Yuan J, Ji Z, Li C, Li Z, Xiao L, et al. Experimental study of the $(4)0^-$ short-range electronic state of the $^{85}Rb^{133}Cs$ molecule by high resolution photoassociation spectroscopy. J Quant Spectrosc Ra 2016;184:8–13. doi:10.1016/j.jqsrt.2016.06.025.

[43] Shimasaki T, Kim J-T, DeMille D. Production of RbCs molecules in the rovibronic ground state via short-range photoassociation to the $2^1\Pi_1$, $2^3\Pi_1$, and $3^3\Sigma_1^+$ states. Chem Phys Chem 2016;17:3677. doi:10.1002/cphc.201600933.

[44] Shimasaki T, Kim J-T, Zhu Y, DeMille D. Continuous production of rovibronic-ground-state rbcs molecules via short-range photoassociation to the $b^3\Pi_1 - c^3\Sigma_1^+ - B^1\Pi_1$ states. Phys Rev A 2018;98:043423. doi:10.1103/PhysRevA.98.043423.

[45] Liu Y, Gong T, Ji Z, Wang G, Zhao Y, Xiao L, et al. Production of ultracold $^{85}Rb^{133}Cs$ molecules in the lowest ground state via the $B^1\Pi_1$ short-range state. J Chem Phys 2019;151:084303. doi:10.1063/1.5108637.

[46] Allouche AR, Korek M, Fakherddin K, Chaalan A, Dagher M, Taher F, et al. Theoretical electronic structure of RbCs revisited. J Phys B 2000;33:2307. doi:10.1088/0953-4075/33/12/312.

[47] Ji Z, Yuan J, Yang Y, Zhao Y, Xiao L, Jia S. Photoionization spectrum of $^{85}RbCs$ molecules produced by short range photoassociation. J Quant Spectrosc Ra 2015;166:36. doi:10.1016/j.jqsrt.2015.07.008.

[48] Ji Z, Li Z, Gong T, Zhao Y, Xiao L, Jia S. Rotational population measurement of ultracold $^{85}Rb^{133}Cs$ molecules in the lowest vibrational ground state. Chin Phys Lett 2017;34:103301. doi:10.1088/0256-307X/34/10/103301.

[49] Li Z, Gong T, Ji Z, Zhao Y, Xiao L, Jia S. A dynamical process of optically trapped singlet ground state $^{85}Rb^{133}Cs$ molecules produced via short-range photoassociation. Phys Chem Chem Phys 2018;20:4893. doi:10.1039/C7CP07756D.

[50] Bergeman T, Kerman AJ, Sage J, Sainis S, DeMille D. Prospects for production of ultracold $X^1\Sigma^+$ RbCs molecules. Eur Phys J D 2004;31:179. doi:10.1140/epjd/e2004-00155-6.

[51] Beuc R, Movre M, Horvatić B, Pichler G. Predictions of absorption bands for RbCs on helium clusters. Chem Phys Lett 2007;435:236. doi:10.1016/j.cplett.2006.12.099.

[52] Kim B, Yoshihara K. Resonance enhanced two photon ionization spectroscopy of RbCs in a very cold molecular beam. J Chem Phys 1994;100:1849. doi:10.1063/1.466536.

[53] Yoon Y, Lee Y, Kim T, Ahn JS, Jung Y, Kim B. High resolution resonance enhanced two photon ionization spectroscopy of RbCs in a cold molecular beam. J Chem Phys 2001;114:8926. doi:10.1063/1.1361251.

[54] Kim B, Yoshihara K. $^3\Delta - ^1\Sigma^+$ transition of RbCs observed in a very cold molecular beam. J Chem Phys 1993;212:271. doi:10.1016/0009-2614(93)89325-C.

[55] Lee Y, Yoon Y, Lee S, Kim J-T, Bongsoo K. Parallel and coupled perpendicular transitions of RbCs 640 nm system: mass-resolved resonance enhanced two-photon ionization in a cold molecular beam. J Phys Chem A 2008;112:7214. doi:10.1021/jp803360w.

[56] Bernath PE. Spectra of atoms and molecules. Oxford University Press; 1995.

[57] Gustavsson T, Amiot C, Vergès J. LIF Spectroscopy of RbCs using an Ar^+ laser. rotational analysis of the $^1\Sigma^+$ ground state for v'' up to 66. Chem Phys Lett 1988;143:101. doi:10.1016/0009-2614(88)87019-2.

[58] Fellows CE, Gutterres RF, Campos APC, Vergès J, Amiot C. The RbCs $X^1\Sigma^+$ ground electronic state: new spectroscopic study. J Mol Spectrosc 1999;197:19. doi:10.1006/jmsp.1999.7880.

[59] Gustavsson T, Amiot C, Vergès J. Spectroscopic investigations of the diatomic molecule RbCs by means of laser-induced fluorescence II. rotational analysis of five excited electronic states. Mol Phys 1988;64:293. doi:10.1080/00268978800100223.

[60] Pavolini D, Gustavsson T, Spiegelmann F, Daudey JP. Theoretical study of the excited states of the heavier alkali dimers: I. the RbCs molecule. J Phys B 1989;22:1721. doi:10.1088/0953-4075/22/11/007.

[61] Fahs H, Allouche AR, Korek M, Aubert-Frécon M. The theoretical spin-orbit structure of the RbCs molecule. J Phys B 2002;35(6):1501. doi:10.1088/0953-4075/35/6/307.

[62] Zaitsevskii A, Pazyuk EA, Stolyarov AV, Docenko O, Klincare I, Nikolayeva O, et al. Permanent electric dipoles and Λ-doubling constants in the lowest $^1\Pi$ states of rbcs. Phys Rev A 2005;71:012510.

[63] Lim IS, Lee WC, Lee YS, Jeung G-H. Theoretical investigation of RbCs via two-component spin-orbit pseudopotentials: spectroscopic constants and permanent dipole moment functions. J Chem Phys 2006;124:234307. doi:10.1063/1.2204607.

[64] Souissi H, Jellali S, Maha C, Habli H, Oujia B, Gadéa FX. An adiabatic spectroscopic investigation of the CsRb system in ground and numerous excited states. J Quant Spectrosc Ra 2017;200:173. doi:10.1016/j.jqsrt.2017.06.009.

[65] LeRoy RJ. RKR1: a computer program implementing the first-order RKR method for determining diatomic molecule potential energy functions. J Quant Spectrosc Ra 2016;186:158. doi:10.1016/j.jqsrt.2016.03.030.